

Fractal Structure of the Harper Map Phase Diagram from Topological Hierarchical Classification

P. Castelo Ferreira¹

ABSTRACT

It is suggested a topological hierarchical classification of the infinite many Localized phases figuring in the phase diagram of the Harper equation for anisotropy parameter ϵ versus Energy E with irrational magnetic flux ω . It is also proposed a rule that explain the fractal structure of the phase diagram. Among many other applications, this system is equivalent to the Semi-classical problem of Bloch electrons in a uniform magnetic field, the Azbel-Hofstadter model, where the discrete magnetic translations operators constitute the quantum algebra $U_q(sl_2)$ with $q^2 = e^{i2\pi\omega}$. The magnetic flux is taken to be the golden mean $\omega^* = (\sqrt{5} - 1)/2$ and is obtained by successive rational approximants $\omega_m = F_{m-1}/F_m$ with F_m given by the Fibonacci sequence F_m . [OUTP-00-08S, cond-mat/0011396]

Keywords: Topological Classification, Harper, Azbel-Hofstadter, Phase Diagram, Fractal, Quantum Groups

PACS: 03.65.Sq, 05.45.+b, 71.23.Ans

¹Adrss. for original paper: Dept. of Physics, Th. Phys., University of Oxford, Oxford OX1 3NP, U.K.
 Curr. Adrss.: Dept. de Fís., Univ. da Beira Interior, Av. Marquês D'Ávila e Bolama, 6201-001 Covilhã
 Curr. Adrss.: CENTRA, IST, Av. Rovisco Pais, 1049-149 Lisboa, Portugal

1 Introduction

In this article we study the phase diagram $E \times \epsilon$ of the Harper equation [2]

$$\begin{aligned}\psi_{n+1} + \psi_{n-1} + 2\epsilon \cos(2\pi\phi_n)\psi_n &= E\psi_n, \\ \phi_n &= \phi_0 + \omega n.\end{aligned}\tag{1}$$

The Harper equation is a Schrödinger operator of two discrete variables ψ and ϕ and, among other application, is associated with the quantum algebra of discrete magnetic translations $U_q(sl_2)$. Namely it is obtained in the Azbel-Hofstadter model [3, 4] of Bloch electrons (electrons on a 2-dimensional periodic potential) in the presence of a uniform magnetic field in the Landau gauge. Here the anisotropy parameter ϵ is the ratio between the spacing in the two directions of the underlying 2-dimensional periodic potential lattice, ω is the magnetic flux per unit cell of the potential lattice and the quantum deformation parameter is $q^2 = e^{i2\pi\omega}$ [3, 7].

The Harper equation is second order on ψ . In order to simplify the numerical treatment of this equation we can cast it into a first order equation by considering the transformation of variables $x_n = \psi_{n-1}/\psi_n$. The resulting equation is equivalent to the Harper equation (1) and is known as the Harper map [8]

$$\begin{aligned}x_{n+1} &= \frac{-1}{x_n - E + 2\epsilon \cos(2\pi\phi_n)}, \\ \phi_n &= \phi_0 + \omega n.\end{aligned}\tag{2}$$

In order to study the phase diagram $E \times \epsilon$ we need to identify the Localized and Extended phases. In order to do so we use Aubry and André study [5], they proved that the Lyapunov exponent λ is proportional to the localization length, specifically $\lambda = -2\gamma$. For the Harper map $\lambda \leq 0$, such that for $\lambda = 0$ the phase is Extended and for $\lambda < 0$ the phase is Localized. The Lyapunov exponent corresponding to the ϕ dynamics is always 0 and the one concerning to the x dynamics is given by

$$\lambda = \lim_{N \rightarrow \infty} \frac{1}{N} \sum_{n=0}^N y_n, \tag{3}$$

where $y_n = \log \frac{\partial x_{n+1}}{\partial x_n} = \log x_{n+1}^2$.

There exists already in the literature classifications, both for the Extended phases [9] and for the Localized phases [11] of equations (1) and (2). In the remaining of this article we propose a new hierarchical topological classification of the several Localized phases for irrational flux $\omega^* = (\sqrt{5} - 1)/2$ based on the topological winding number of the attractors on the space of variables (ϕ, x) . In order to study the irrational phase diagram we take successive rational approximants ω_m . The fractal structure of the phase diagram emerge naturally in this framework and we suggest a rule that reproduces it. As we will show in detail, the great advantage of this new classification is that its labels correspond to the magnitude of the several different phases. Here the phase magnitude is understood as the area of each different phase on the full phase diagram. Also the area (hence magnitude) of

the several phases coincide with its order of appearance in the phase diagrams for successive approximants ω_m to ω^* .

This article is organized as follows, in section 2 we introduce the irrational phase diagram and successive approximants as well as the one-dimensional attractor in the $\phi \times x$ diagram for irrational ω^* . In section 3 we justify the identification of the $\phi \times x$ with a torus and introduce our classification. In section 4 we analyse the phase diagram and give the rules to build the Hierarchical Tree for the phase diagram. In order to better explain the fractal structure and how to build this Tree we have three appendixes. In appendix A we present the Lyapunov exponents for $\omega = \omega^*$ and $\epsilon = 1$ with enough resolution to identify the several phases (that correspond to each negative *bump*). In appendix B we list the $\phi \times x$ diagrams up to $\eta = 55$ (with indication of the respective energies). Finally in appendix C we show graphically how to build the triangular structure up to level 9.

2 Phase Diagram

We proceed to present the numerical results and study the properties of the $E \times \epsilon$ phase diagram of the Harper map (2) which is equivalent to the Harper equation (1). We consider successive rational approximants $\omega = \omega_m$ of the irrational value $\omega = \omega^*$ given by the golden mean. The rational succession $\omega_m = F_{m-1}/F_m$ converges to the irrational golden mean $\omega^* = (\sqrt{5} - 1)/2$. Being $F_0 = F_1 = 1$ and $F_m = F_{m-1} + F_{m-2}$ the m^{th} Fibonacci number in the Fibonacci sequence.

Computing the phase diagram for successive rational ω_m allows us to *visualize* the fractal

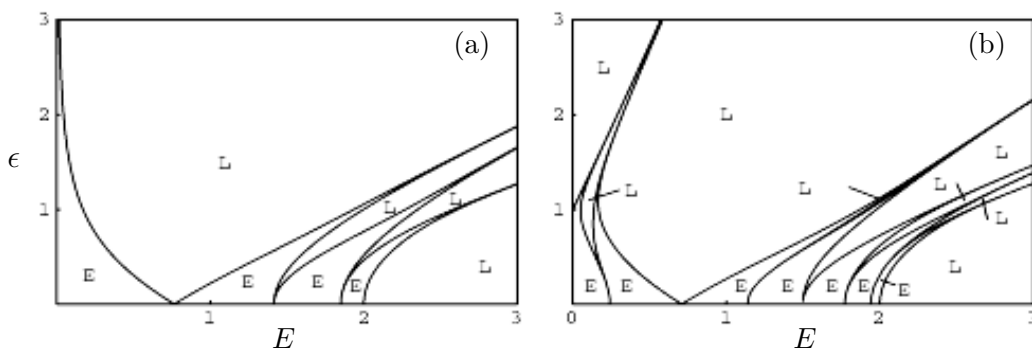


Figure 1: Phase diagram for rational ω for $\phi_0 = 0$. The Localized phases (L) are presented. (a) $\omega_5 = 5/8$; (b) $\omega_6 = 8/13$.

and denser. In the limit of irrational ω^* , the lines cross at the critical value $\epsilon = 1$ and the Lyapunov exponents go to zero at these points of intersection [10]. Although for the rational values ω_m the phase diagrams depend on ϕ_0 , in the irrational limit ω^* the phase diagram is not sensitive to ϕ_0 . Note also that for $\epsilon > 1$ the Lyapunov exponents become always negative, this means that the phase transitions are smooth without undergoing an

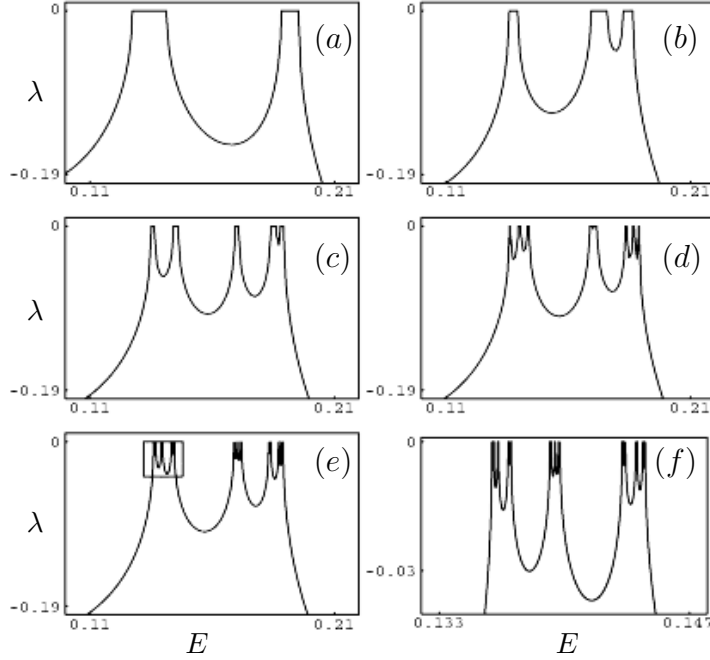


Figure 2: Fractalization of the phase diagram. Lyapunov exponents λ for $\epsilon = 1$ and $\phi_0 = 0$. (a) $\omega_7 = 13/21$; (b) $\omega_8 = 21/34$; (c) $\omega_9 = 34/55$; (d) $\omega_{10} = 55/89$; (e) $\omega = \omega^* = (\sqrt{5} - 1)/2$; (f) $\omega = \omega^*$, zoom of (e).

Extended phase. See [11] for further details in these discussion. As a final remark we note that the phase diagram is symmetric with respect to both axes $E = 0$ and $\epsilon = 0$. Also we stress that from the mathematical point of view the parameters E and ϵ can be both negative or positive, from a physical point of view they should be positive, E is the energy and ϵ is the ratio of the unit cell sides. The phase diagram becomes in the limit of irrational ω^* a fractal (see figure 2 and 3), more exactly, a Cantor set [6]. It is this particular limit that interest us. From the above discussion it is enough to restrict our analysis of the several phases to the first quadrant for $\epsilon < 1$ and $\phi_0 = 0$.

It remains to study the attractors in the space of variables (ϕ, x) . Concerning the purpose of this work we describe the behaviour of the map in the Localized phases only, for further details on extended phases see [9, 11]. For a given ω_m , the map has 0-dimensional attractors with period F_m , this means that the attractor is a F_m -cycle. In other words the map iteration cycle trough F_m distinct points. In the limit $\omega \rightarrow \omega^*$ it becomes an one-dimensional attractor F_∞ , it is a line. These results are present in figure 4. It is this property that we are exploring next in order to define our phase classification.

3 Topological Classification

It is time to define the classification. We are considering a map from the generic space of variables $\phi \times x$ to a torus such that the identifications $\phi : 0 \cong 1$ and $x : +\infty \cong -\infty$ hold. We note that we don't actually have to impose these identifications, they naturally come

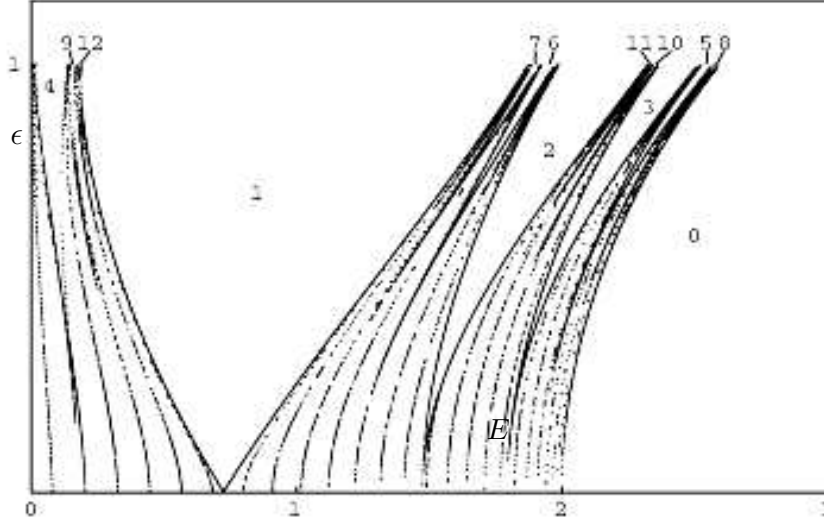


Figure 3: Phase diagram for ω^* . The first 12 zones are labeled in the diagram.

from the definitions of the variables ϕ and x .

The ϕ identification is justified by noting that $2\pi\phi$ is an angular phase, then the variable ϕ is compact in the interval $[0, 1]$ with identification $\phi : 0 \cong 1$ as any usual angular variable.

The x identification $x : +\infty \cong -\infty$ is somehow more subtle. By inspecting the attractors we realize that the one-dimensional attractors cross from $\pm\infty$ to $\mp\infty$ at the same value of ϕ (as an example see figures 4 and 5). The $\phi \times x$ diagram gives us local properties of the original continuous variable ψ at each spatial index n . We note however that we completely loose all the information about the spatial localization itself (ordering on the spatial indexes n) of where (and in which order) the original variable ψ have those properties. We are going to show that the $x_n = \psi_{n-1}/\psi_n$ variable is describing exactly the same situation for both cases $x = +\infty$ and $x = -\infty$. The setup here is the original continuous variable being null $\psi = 0$ at some (or many) points, $x_n = \psi_{n-1}/\psi_n = \pm\infty$ means that $\psi_n = 0$. To show the validity of this statement based on geometrical arguments see figure 6 where two points, at different spatial localizations n and n' , are considered, the discretized points ψ_{n-1} , ψ_n , $\psi_{n'-1}$ and $\psi_{n'}$ are represented in the figure. Take in both cases $|\psi_{n-1}| \gg |\psi_n|$ and $|\psi_{n'-1}| \gg |\psi_{n'}|$. This means that $x_n \sim +\infty$ and $x'_{n'} \sim -\infty$ do correspond to the same situation of the continuous variable $\psi = 0$. Both kind of situations will always occur for irrational ω (many times for large N) because the period of the variable ψ and the period of the underlying discretized lattice (given by the magnetic flux ω) are *incommensurate* [3, 4, 10].

In order to formalize our argument we can invert the map $x_n = \psi_{n-1}/\psi_n$ between variables obtaining $\psi_n = \psi_{n-1}/x_n$, then we have that $x_n \rightarrow \pm\infty$ correspond to one only value $\psi_n \rightarrow 0$. Although not in the scope of the present study, it is interesting to note that $x_n \rightarrow 0$ correspond to $\psi_n \rightarrow \pm\infty$, therefore a divergence of the original variable ψ .

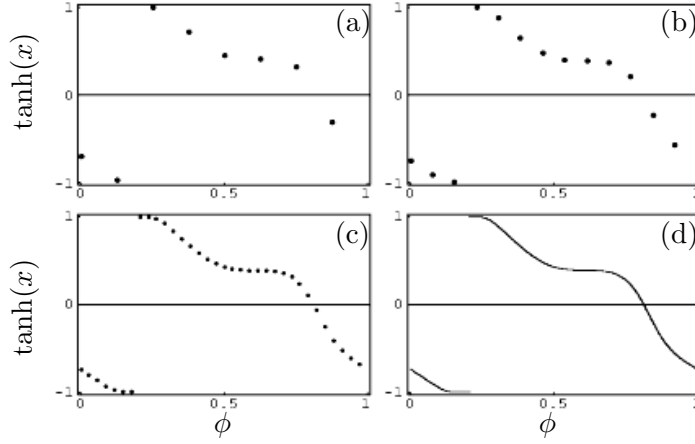


Figure 4: Attractors in the space of variables $\phi \times x$ corresponding to the Localized phase 1, for $\phi_0 = 0$, $E = 0.75$ and $\epsilon = 0.5$. (a) $\omega_5 = 5/8$; (b) $\omega_6 = 8/13$; (c) $\omega_{11} = 89/144$; (d) $\omega = \omega^* = (\sqrt{5} - 1)/2$, in this limit the F_m -cycle becomes a line.

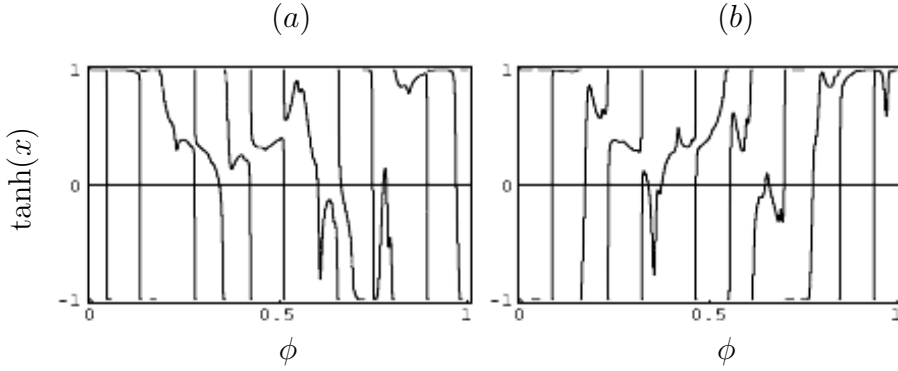


Figure 5: Maps for ω^* and $\epsilon = 1$. (a) $\eta = 11$, $E = 2.342$; (b) $\eta = 10$, $E = 2.347$.

So we just proved that the variable identifications $\phi : 0 \cong 1$ and $x : +\infty \cong -\infty$ are natural with out need for any *a priori* assumptions. Then the space of variables $\phi \times x$ is topologically a torus. Therefore the one-dimensional attractors, for irrational ω^* , are close contours living on the surface of that torus. By inspection we conclude that the attractors wind several times along the x coordinate. Furthermore the winding number along the x homology cycle is unique for each continuous Localized phase. So we classify these several phases accordingly, such that our classification label η is the winding number along the x homology cycle of the one-dimensional attractors. Note that the winding number in the ϕ homology cycle is always 1 except for $E = 0$ and $\epsilon < 1$ where there are two one-dimensional attractors with winding number 0 in the x axis and 1 in the ϕ axis [10]. This particular case $E = 0$ is excluded from our classification.

The great advantage of this classification is that it also provide us a natural hierarchy based on the areas of the several phases. It coincides with the ordering of the areas occupied by the corresponding Localized phases. Furthermore as we consider successive ω_m 's, the order of appearance of the phases also coincides with their hierarchical importance. As explained

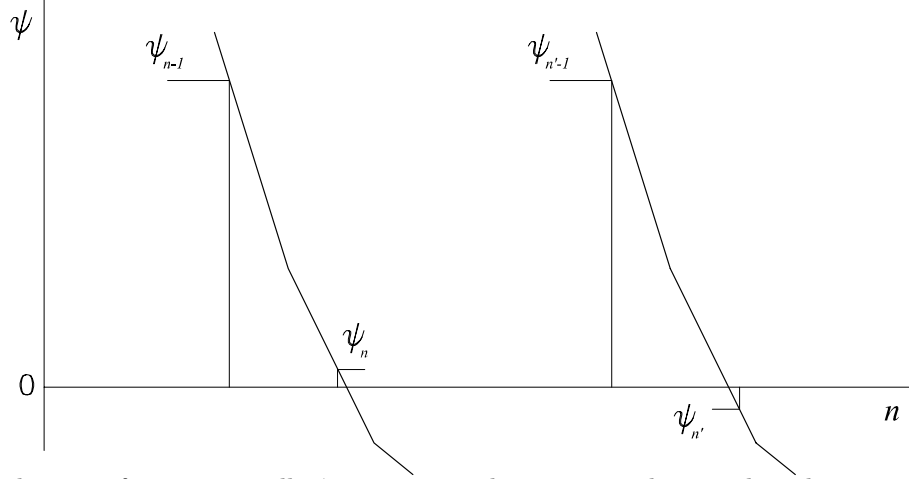


Figure 6: The wave function is null, $\psi = 0$, at two distinct spatial points but the corresponding x have opposite signs.

in section 2 this is due to the Localized phases emerging from the splitting of the Extended phases. The diagram for irrational ω^* and the classification of areas up to $\eta = 12$ is presented in figure 3. As an example for higher η attractors we present in figure 5 the cases for $\eta = 10$ and $\eta = 11$.

4 Hierarchical Fractal Structure

Here we will define the generic rules to build the fractal structure of the phase diagram in the first quadrant ($E > 0$ and $\epsilon > 0$).

First let us state some conclusions obtained by inspection (CI) of successive phase diagrams for approximants ω_m (see figures 1 and 3):

- CI.1 In each new diagram for successive approximants the last phase on the far right (for $E > 2$) has always $\eta = 0$ and correspond to the phase with greater area. It is always present and doesn't contribute anything to explain the structure. So **$\eta = 0$ is excluded from the classification.**
- CI.2 The first phase to appear next (corresponding to the next greater area) as we move in the Fibonacci succession, is $\eta = 1$. Although we have two Fibonacci elements corresponding to this number, we have only one phase in the phase diagram. In some way (that we will explain later) this means that **$\eta = 1$ is a degenerate phase.**
- CI.3 We recall from section 2 that for each approximant ω_m there are F_{m-1} Localized phases, from the Fibonacci succession we have that $F_m = F_{m-2} + F_{m-1}$, then as we go trough the approximants, from ω_m to ω_{m+1} emerge exactly F_{m-2} new Localized phases. It seems then a good guess to organize the phases in levels such that in each level $k = m - 1$ there are exactly F_{k-2} labels in the range $F_{k-1} < \eta_{level\ k} \leq F_k$. We are therefore building a **triangular structure.**

- CI.4 Also as we increase m the last phase on the far right (just before $\eta = 0$) corresponds always to one label belonging to the Fibonacci succession $\eta_k^R = F_m$ with $k = m - 1$. We will call η_k^R the **right pivots**.
- CI.5 The last phase on the left side of the diagram (near $E = 0$) only changes for the second odd number in the Fibonacci succession (even, odd, *odd*, even, odd, *odd*, ...). This means that only for $k = 3n + 1$ (for all integer n) we will have a label $\eta_{3n+1}^L = F_{3n} + F_{3n-2}$. We will call η_k^L the **left pivots**.
- CI.6 As we move along the approximants new phases will emerge in the bulk of the diagram next to the ones that already exist in the previous approximants. However if one phase η_n appears at some approximant ω_m , at the immediately next approximant ω_{m+1} no new phases will appear next to this phase η_n . So, for each new phase appearing, **there are not adjacent new phases at the immediately next approximant**.
- CI.7 Also these new phases appearing adjacent to the already existing phases in the bulk will appear either on the right or on the left of the already phases that already exist. So the **order of appearance of new phases alternate between left and right**.

So we have a triangular Hierarchical Tree organized in levels, each *level* k has exactly F_{k-2} elements (see point CI.3 above) and we are ready to define the rules to build it. In order to accomplish it we first give the rules for the edges of the triangle and then define a recursive rule for the bulk of the triangle. For the reader interested in the full details we present in appendix A the Lyapunov exponents for $\omega = \omega^*$ and $\epsilon = 1$ with enough resolution to identify the several phases (that correspond to each negative *bump*) and in appendix B we list the $\phi \times x$ diagrams up to $\eta = 55$ with indication of the respective energies.

We can define the vertex and edges of the triangle following the following rules:

- R.I On the top vertex of the triangle is placed the degenerate label $\eta = 1$ (see point CI.2 in our list of conclusions above). It is degenerate simply because it belongs simultaneously to the right and left edge of the triangle, i.e. it is both a left and a right pivot $\eta_0^R = \eta_0^L = 1$ (see conclusions by inspection CI.2, CI.4 and CI.5).
- R.II At the right edge of the triangle we have at each *level* k the right pivots $\eta_k^R = F_{k+1}$ distributed, in sequence (see point CI.4 on the list of conclusions above).
- R.III On the left edge not all levels have a pivot, we will have left pivots only for *level* $(3n+1)$ (for any integer n) with labels $\eta_{3n+1}^L = F_{3n} + F_{3n-2}$ (see figure 7).

Next we will define a recursive rule for the bulk of Tree. In order to distribute the labels in each level, consider the Tree completely built up to *level* k and let us construct the next *level* $k+1$. We have therefore F_{k-1} labels in the range $F_k < \eta_{\text{level } k+1} \leq F_{k+1}$ (see point CI.3). Although we already have rules for the edges of the triangle (see Rule II and Rule III) we include in the recursive rules also the edges. The following rules should be applied in sequence:

- R.1 Group the two last right pivots (η_{k-1}^R, η_k^R) and sum them together, the result is the new pivot of level $k + 1$, i.e. $\eta_{k+1}^R = \eta_{k-1}^R + \eta_k^R$.

R.2 Group in pairs all the remaining elements (the labels) up to level $k - 1$ (we note that no other elements of *level* k will be used except for the right pivot η_k^R). The way to group them is to start from the right pivot η_{k-2}^R and group it with the immediately adjacent element to the left. Then we take the next element immediately adjacent to the left and group it to next one adjacent to the left, and so on. Here adjacent means the order in the phase diagram as we move to the left, in terms of the Hierarchical Tree, i.e. the closest element in relation to the horizontal projected distance. From two in two levels there will be out of the pairs a single left pivot (see point CI.5 above), then after applying Rule R.3 below, apply also Rule R.4.

R.3 Sum the right pivot of *level* k (η_k^R) to all the pairs obtained in Rule 2, then we swap the order of the elements inside each pair and place the resulting (swapped elements) pair at level $k + 1$ between the elements of the original pair. Again, here, between means in relation to the horizontal projection of the elements. We note that these rules do reproduce the behaviour described in the conclusions by inspection CI.6 and CI.7.

R.4 From two in two levels we will have a single left pivot unpaired of *level* $k-1$, in this case we sum it to the right pivot η_k^R and place the result as the left pivot of *level* $k+1$.

We note that in order to apply the recursive rules we only need the two first labels, i.e. $\eta_0^R = \eta_0^L = 1$ and $\eta_1^R = 2$. We note that Rule II is equivalent to Rule 1 and Rule III to Rule 4, we simple list both set for completeness. In this way the rules defining the triangular structure are complete! The first 9 levels of the Hierarchical Tree are shown in figure 7, we can compare it with the corresponding phases in the phase diagram (figure 3). In appendix C we show graphically how to build the triangular structure up to level 9 using these recursive rules.

5 Conclusions

In this paper we have proposed an integer topological hierarchical classification for the infinite many Localized phases in the phase diagram $E \times \epsilon$ of the Harper map for irrational parameter $\omega^* = (\sqrt{5} - 1)/2$. This map is equivalent to the Harper equation which, among other applications, describes the Azbel-Hofstadter model with E being the energy, ϵ the anisotropy parameter and ω the magnetic flux per unit cell. The classification is based in the winding number around the holonomy cycles of the One-dimensional attractors in the toroidal space of variables $\phi \times x$. For the classifications obtained, the fractal structure of the $E \times \epsilon$ phase diagram is built and organized into a triangular structure that exactly describes the phase diagram taking in account the ordering of the several phases. Moreover the integer classification labels (1, 2, 3, ...) exactly correspond to the phase importance, concerning their area in the phase diagram and order of appearance in the succession of phase diagrams for the several approximants ω_n converging to ω^* . So in this since the triangular fractal structure correctly describes all approximants. As possible future works in this subject it would be interesting to investigate the fractal structure for ω given by other irrational numbers and, if possible, to find a rule for generic irrational numbers and respective approximants.

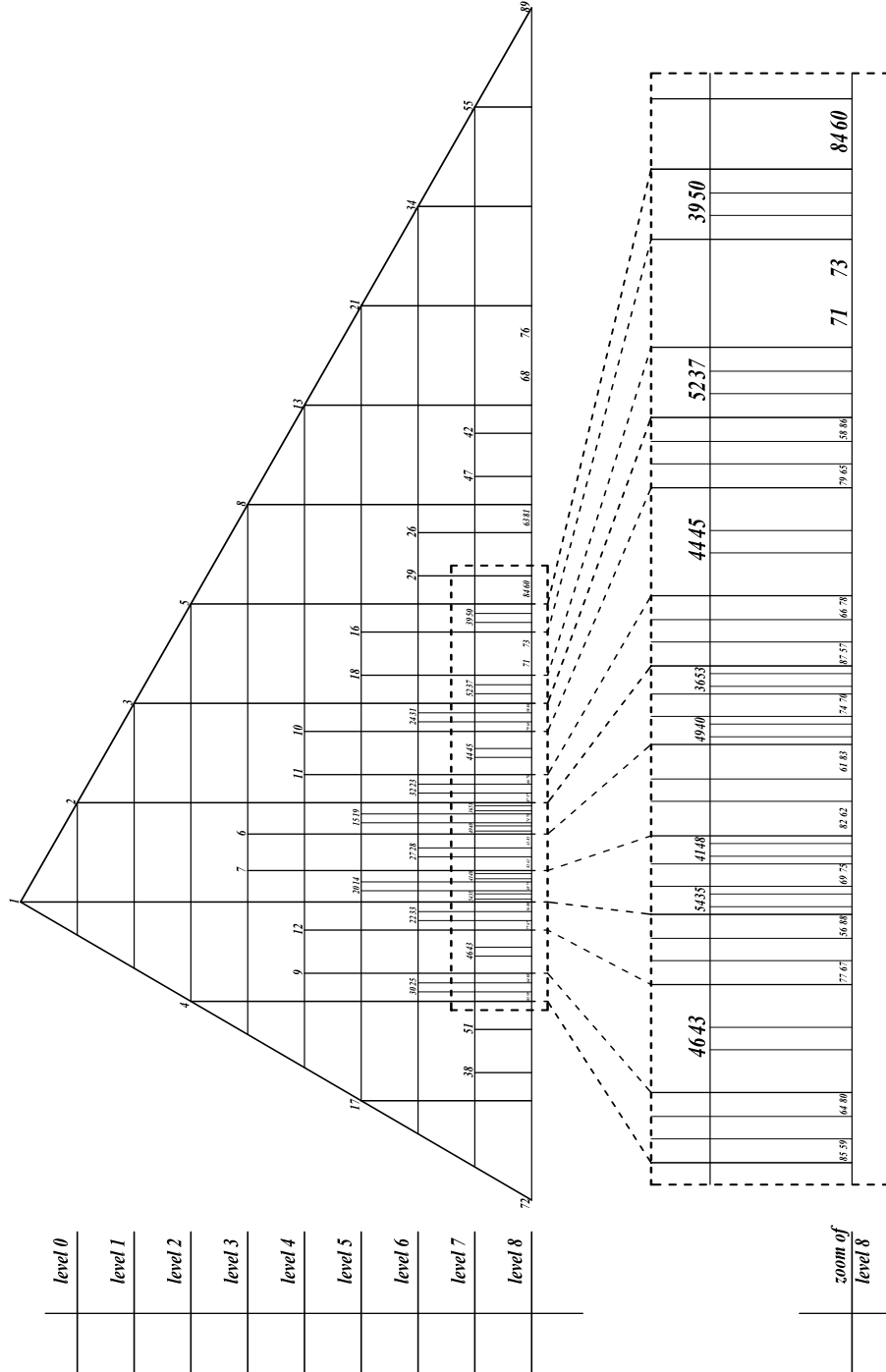


Figure 7: Fractal structure of the phase diagram (to be seen in landscape orientation).

Acknowledgements

This work was supported by PRAXIS XXI/BD/11461/97 and SFRH/BPD/17683/2004. The first part of this work was done at the Department of Physics of the University of Oxford, without the well organized computer resources efficiently available there it would be impossible to accomplish it. The author thanks F.P. Mancini and M.H.R. Tragtenberg for several discussions and comments.

References

- [1] P. Castelo Ferreira, F. P. Mancini and M. H. R. Tragtenberg, unpublished, e-print version 3 of `cond-mat/0006310` (weblink: xxx.lanl.gov/abs/cond-mat/0006310v3).
- [2] P. G. Harper, Proc. Phys. Soc. London **A68**, 874 (1955).
- [3] M. Ya Azbel, Sov. Phys. JETP **19**,634 (1964).
- [4] D. R. Hofstadter, Phys. Rev. **B14**, 2239 (1976).
- [5] S. Aubry and G. André, Ann. Israel Phys. Soc. **3**, 133 (1980).
- [6] J. Bellisard and B. Simon, J. Funct. Anal. **48**, 408 (1982).
- [7] P. B. Wiegmann and A. V. Zabrodin, Nucl. Phys. **B451**, 699 (1995), `cond-mat/9501129`.
- [8] J. A. Ketoja and I. I. Satija, Physica **D109**, 70 (1997).
- [9] A.G. Abanov, J. C. Talstra and P. B. Wiegmann, Nucl. Phys. **B525**, 571 (1998), `cond-mat/9711274`.
- [10] A. Prasad, R. Ramaswamy, I. I. Satija and N. Shah, Phys. Rev. Lett. **83**, 4530 (1999).
- [11] P. Castelo Ferreira, F. P. Mancini and M. H. R. Tragtenberg, Phys. Lett. **A296** (2002) 91, `cond-mat/0011239`.

A Lyapunov Exponent

In this appendix we present the Lyapunov exponents for $\epsilon = 1$ and ω^* . The several phases are labelled until $\eta = 55$.

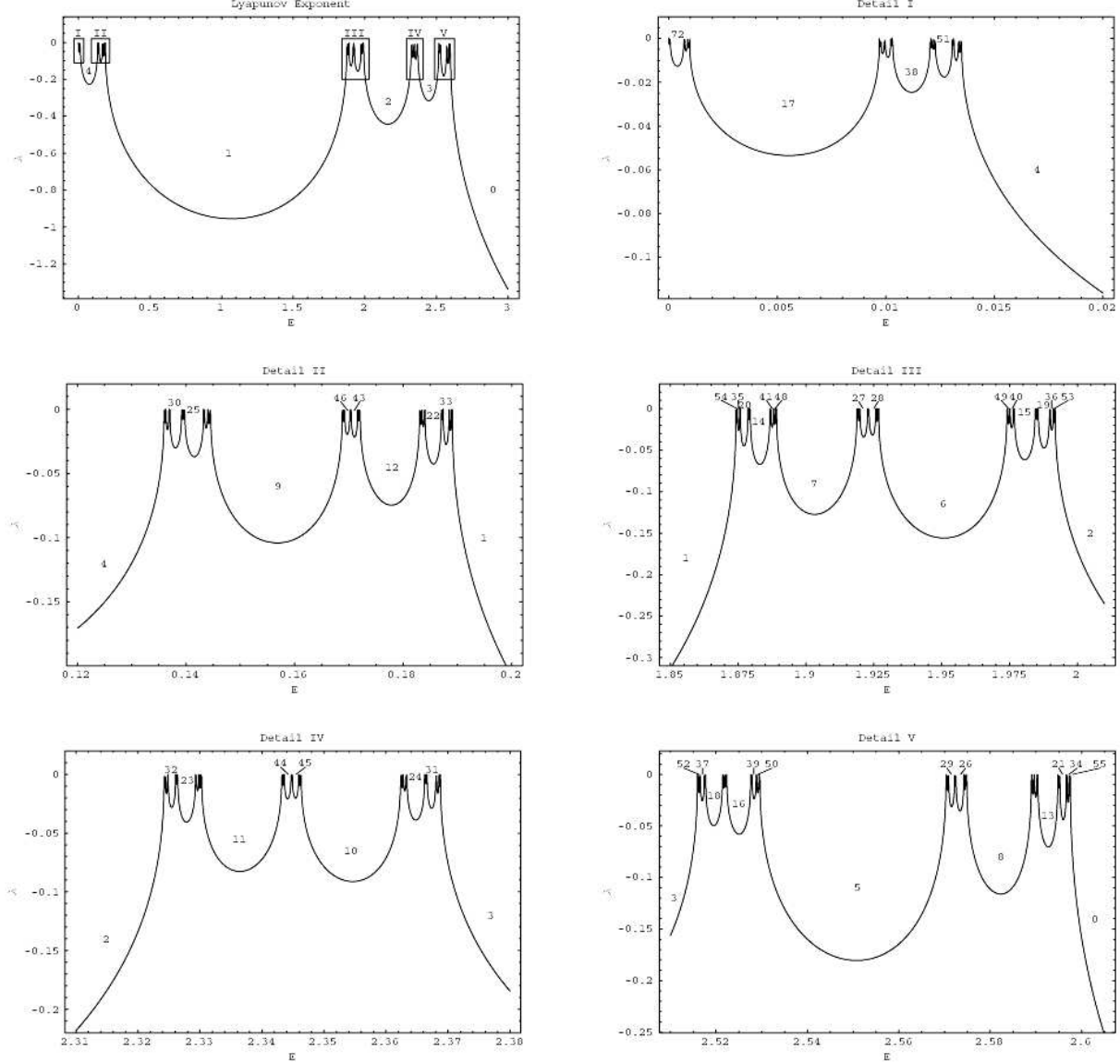


Figure 8: Lyapunov exponent λ as a function of energy E for $\epsilon = 1$ and $\omega = \omega^*$. The Details I to V correspond to the marked regions in the first graph.

B $\phi \times x$ diagrams

Next we list all the attractors in the space of variables $\phi \times x$ up to $\eta = 55$.

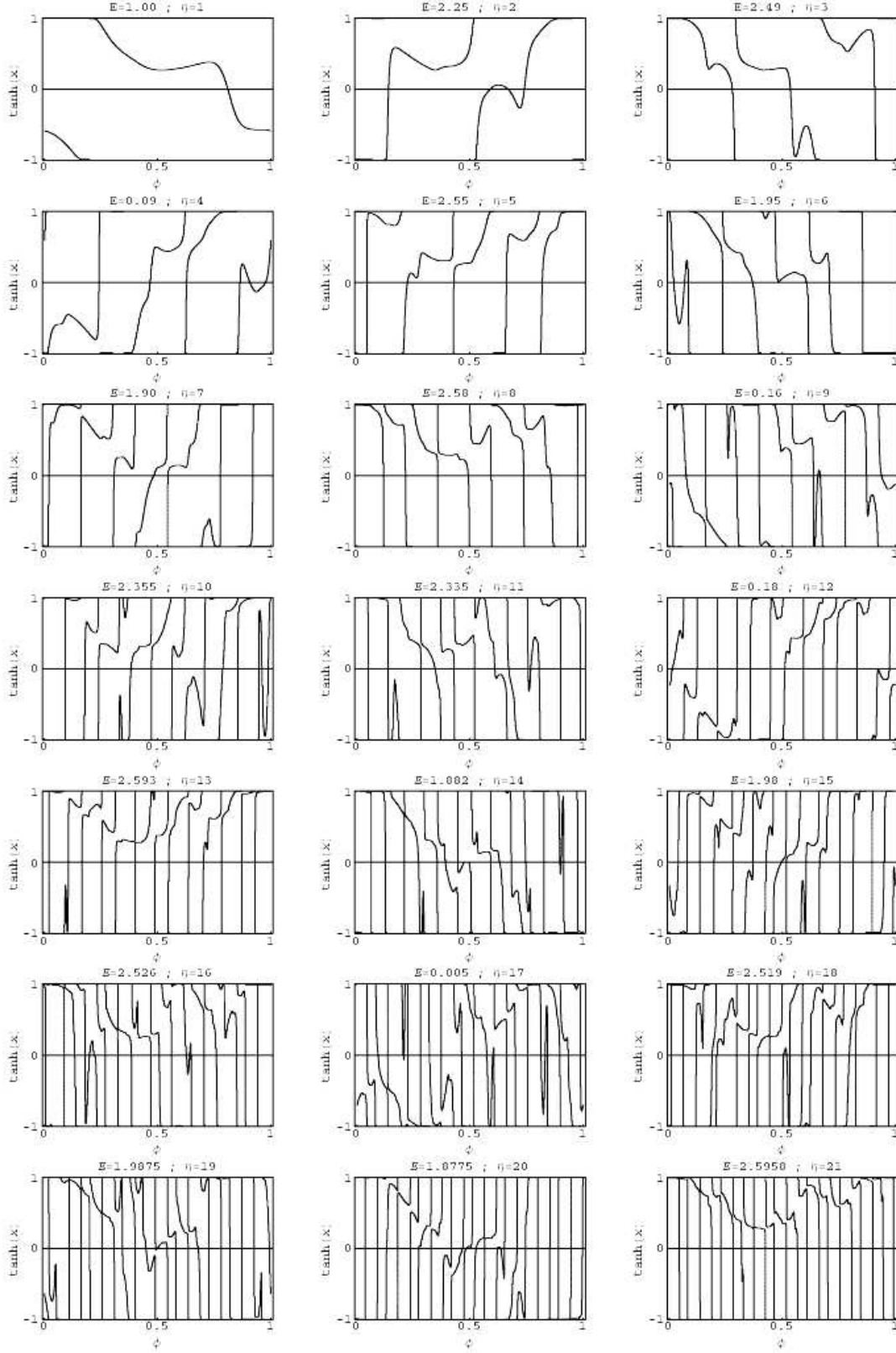


Figure 9: Attractors in the space of variables $\phi \times x$ up to $\eta = 21$.

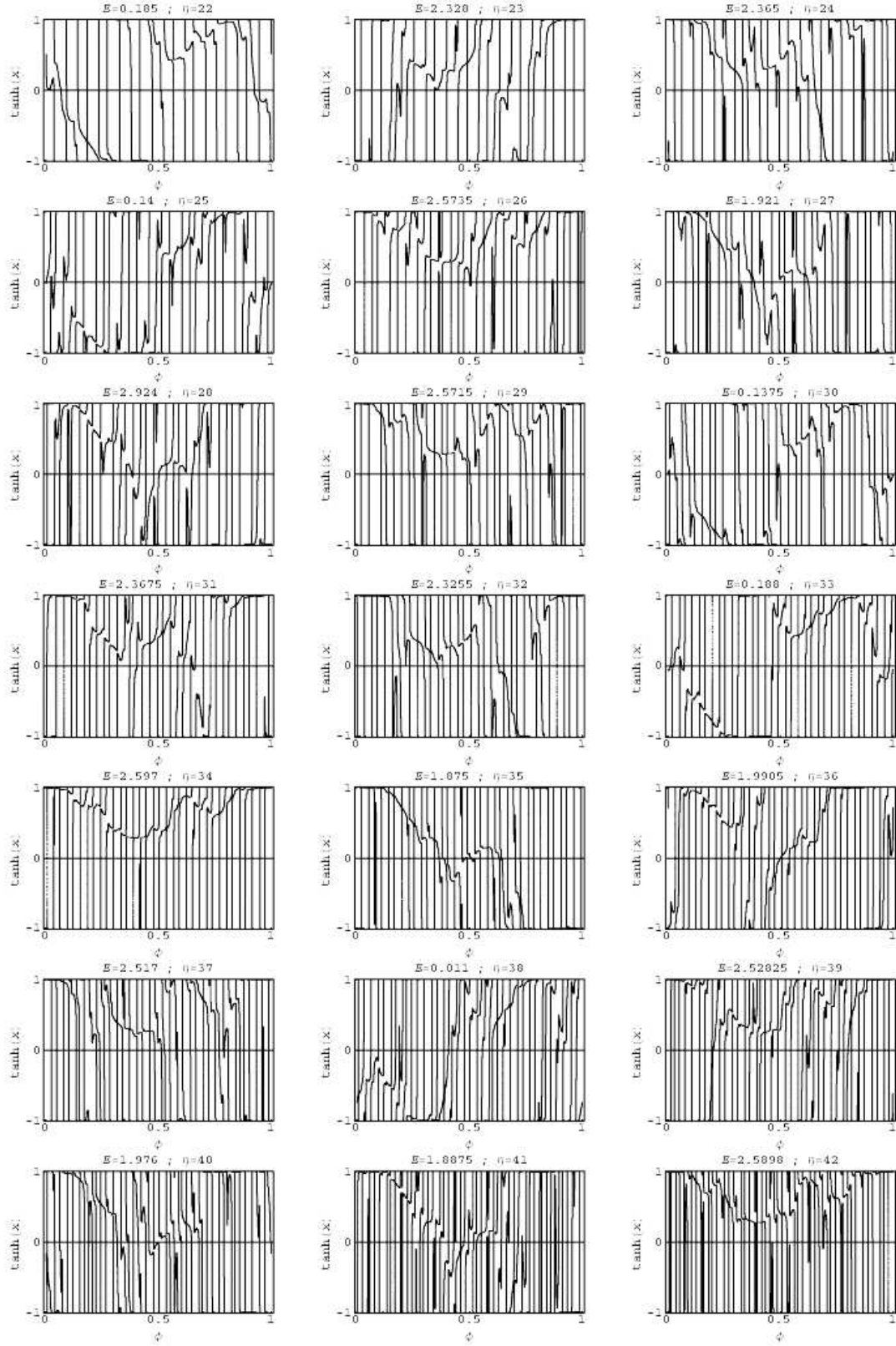


Figure 10: Attractors in the space of variables $\phi \times x$ from $\eta = 22$ to $\eta = 42$.

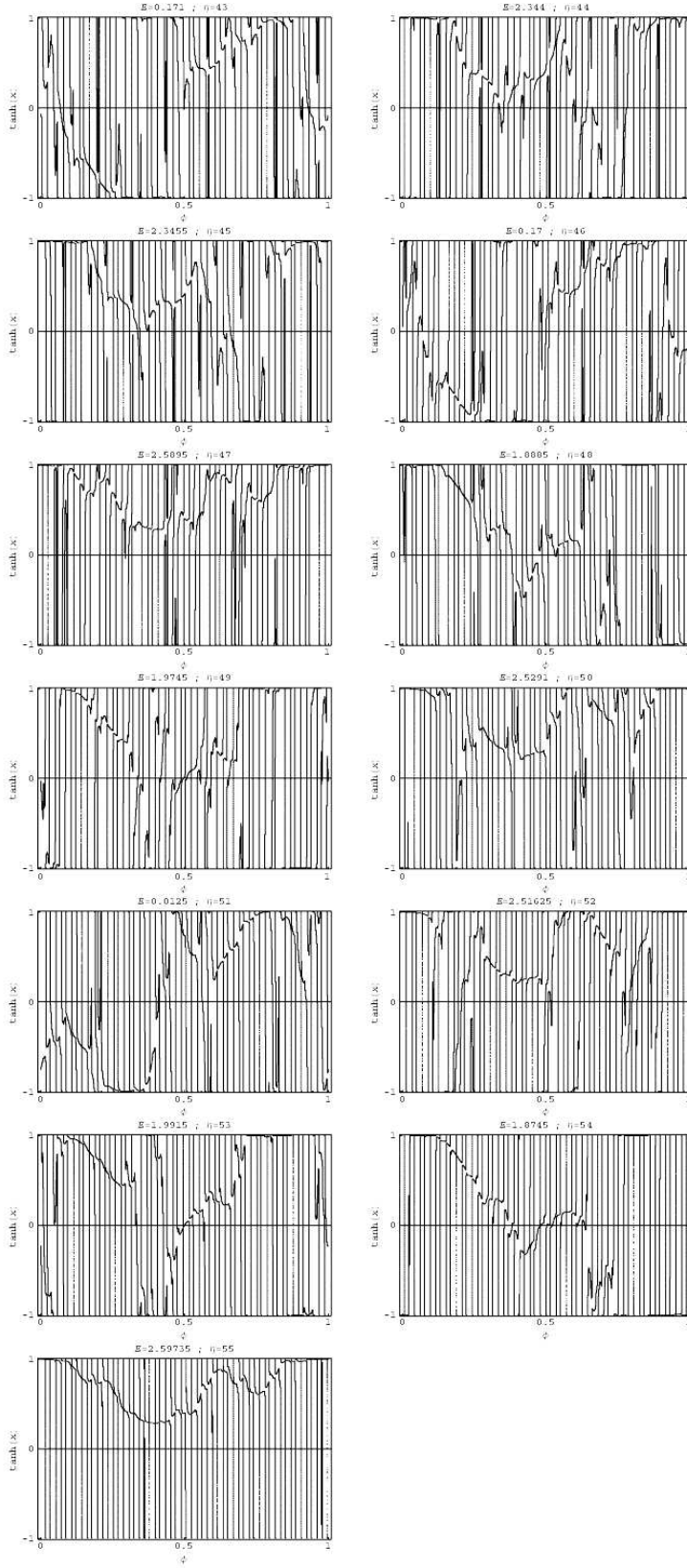


Figure 11: Attractors in the space of variables $\phi \times x$ from $\eta = 43$ to $\eta = 55$.

C Building the Hierarchical Tree

We show graphically how to build the Hierarchical Tree up to *level 9*. *Level 1* and *Level 2* are given and only contain the vertex (simultaneously left and right) pivot $\eta_0^R = \eta_0^L = F_1 = 1$ and the right pivot $\eta_1^R = F_2 = 2$. We give details of the application of the construction rules up to *level 6* which contains all rules. The remaining levels do not involve any new rule and can be build straight forwardly.

On the following figures the pivot used to construct each level $n + 1$ (i.e. η_n^R , the pivot of the level immediately above the one we are constructing) is inside a darker circle. The remaining elements used are grouped in pairs pictorially marked. We note that up to some *level n* we have present in our Tree all labels up to $\eta_n^R = F_{n+1}$.

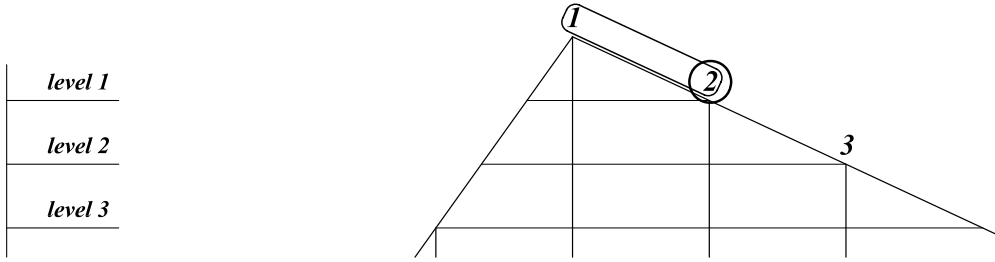


Figure 12: Building *level 2* ($n + 1 = 2$). The right pivot at level $n = 1$ is $\eta_1^R = F_2 = 2$. The next pivot is obtained by adding the two previous pivots $\eta_2^* = \eta_0^R + \eta_1^R = F_1 + F_2 = 1 + 2 = 3$. There are no more elements in this level.

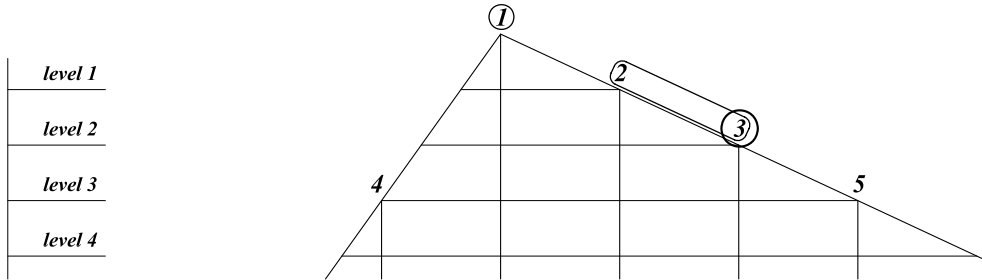


Figure 13: Building *level 3* ($n + 1 = 3$). The pivot at level $n = 2$ is $\eta_2^R = F_3 = 3$. The next pivot is obtained by adding the two previous pivots $\eta_3^R = \eta_1^* + \eta_2^* = 2 + 3 = 5$. There are not enough elements to group in pairs, we have one single element at the vertex of the triangle $\eta_0^L = \eta_0^R = F_1 = 1$ that we deal as being a left pivot. Then we sum it the right pivot of *level 2* η_2^R obtaining the new left pivot $\eta_3^L = \eta_0^L + \eta_2^R = F_1 + F_3 = 1 + 3 = 4$.

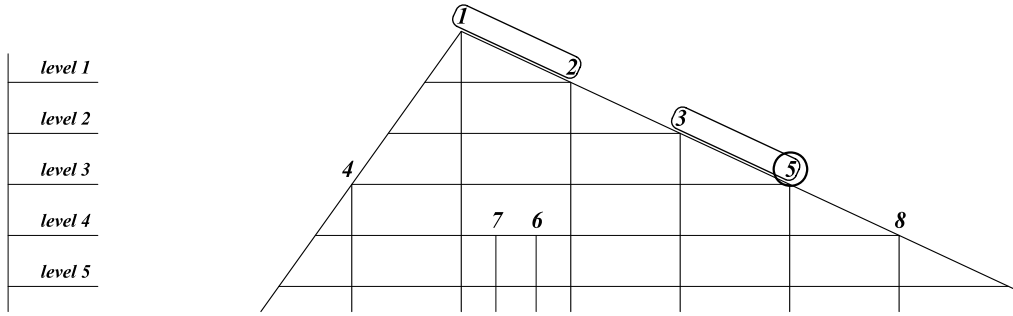


Figure 14: Building *level 4* ($n + 1 = 4$). The pivot at level $n = 3$ is $\eta_3^R = F_4 = 5$. The next pivot is obtained by adding the two previous pivots $\eta_4^R = \eta_2^* + \eta_3^* = 3 + 5 = 8$. The remaining elements on the levels above (not including) *level 3* are grouped in pairs, we obtain one single pair (1, 2). We sum this pair to the current level pivot $\eta_3^R = 5$ and place the resulting pair with the order of the elements reversed below and between the elements of the original pair (1, 2). This means we obtain the pair (7, 6) and place it as shown in the figure.

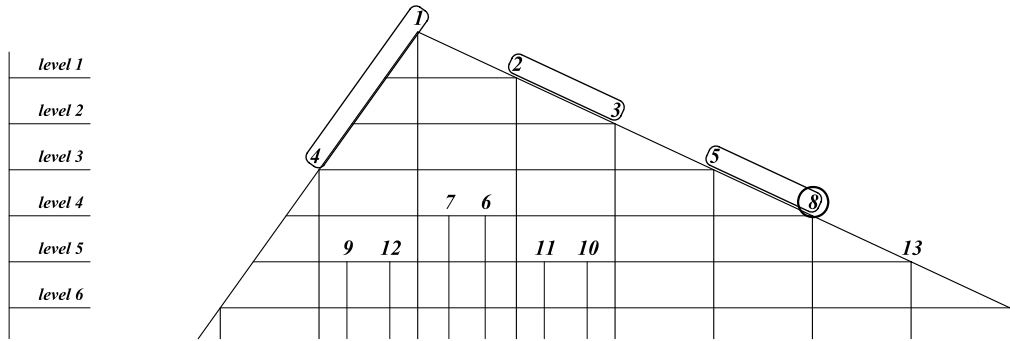


Figure 15: Building *level 5* ($n + 1 = 5$). The pivot at level $n = 4$ is $\eta_4^R = F_5 = 8$. The next pivot is obtained by adding the two previous pivots $\eta_5^R = \eta_3^* + \eta_4^* = 5 + 8 = 13$. The remaining elements on the levels above (not including) *level 4* are grouped in pairs, we obtain two pairs (4, 1) and (2, 3). We sum these pairs to the current level pivot $\eta_4^R = 8$ and place the resulting pairs with the order of the elements reversed below and between the elements of the original pairs. This means we obtain the pairs (9, 12) and (11, 10) and place them as shown in the figure.

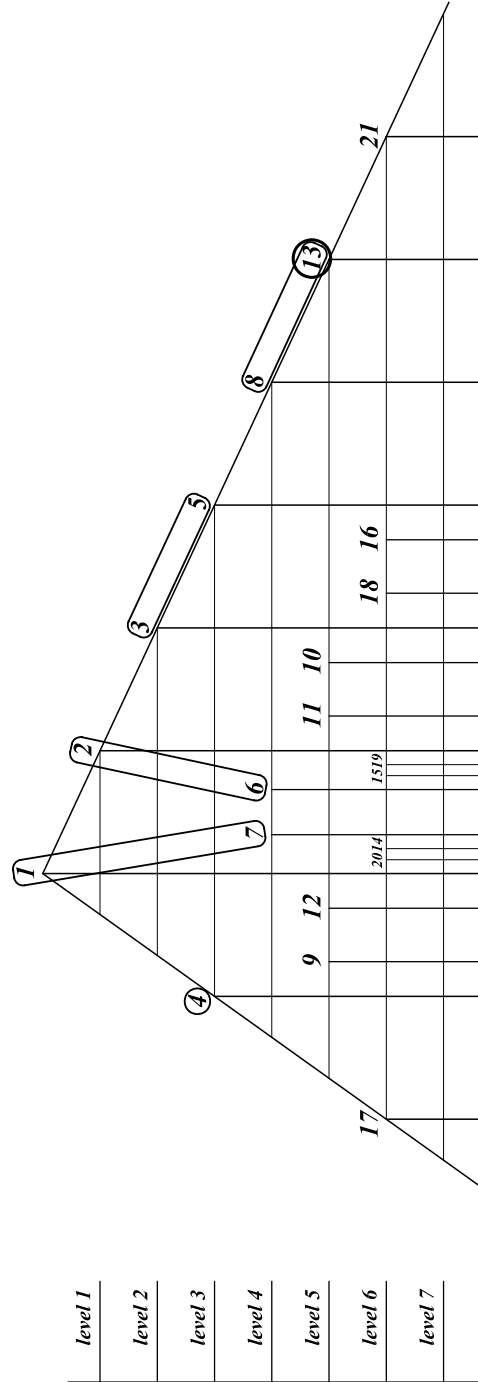


Figure 16: Building *level 6* ($n + 1 = 6$). The pivot at level $n = 5$ is $\eta_5^R = F_6 = 13$. The next pivot is obtained by adding the two previous pivots $\eta_5^R = \eta_3^* + \eta_4^* = 8 + 13 = 21$. The remaining elements on the levels above (not including) *level 5* are grouped in pairs from right to left. As expected for *level 6* we have one lonely left pivot $\eta_3^L = 4$ and we obtain three pairs $(1, 7)$, $(6, 2)$ and $(3, 5)$. We sum the current level pivot $\eta_5^R = 13$ to the lonely left pivot obtaining the new left pivot $\eta_6^L = \eta_5^R + \eta_3^L = 13 + 4 = 17$. As for the three pairs we sum them to the current level pivot $\eta_5^R = 13$ and place the resulting pairs with the order of the elements reversed below and between the elements of the original pairs. This means we obtain the pairs $(20, 14)$, $(15, 19)$ and $(18, 16)$ and place them as shown in the figure (to be seen in landscape orientation).

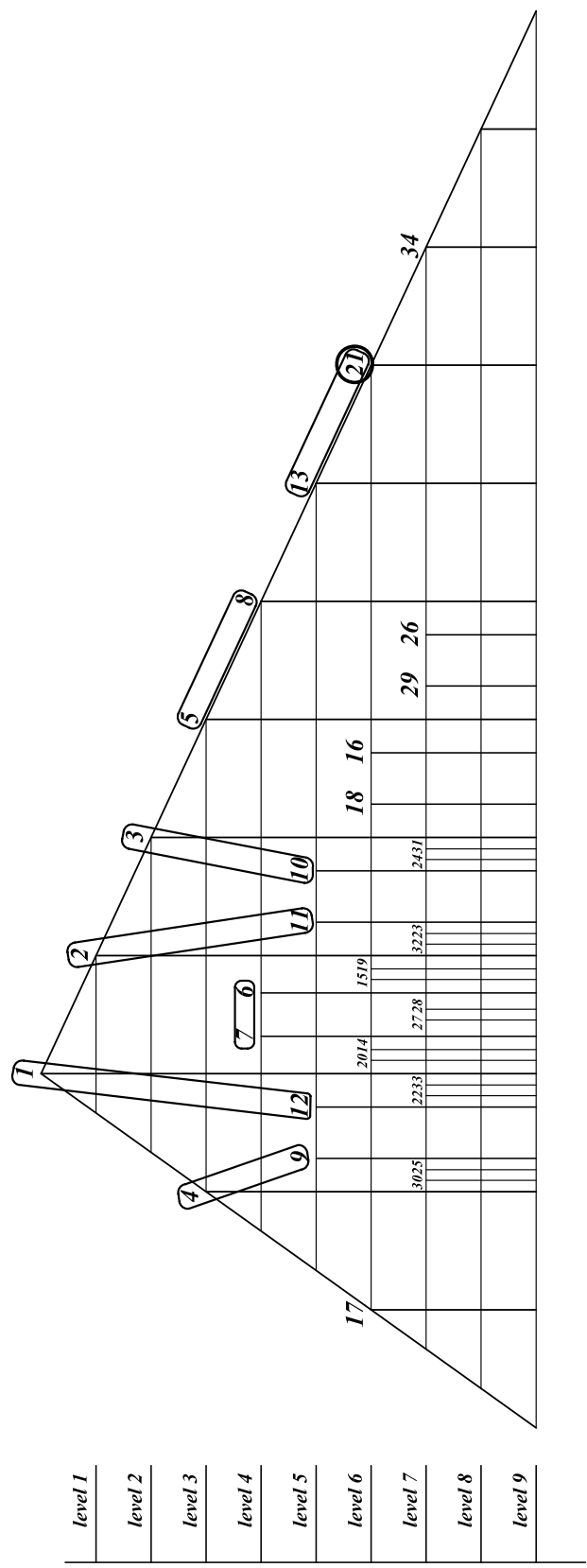


Figure 17: Building level 7 (to be seen in landscape orientation).

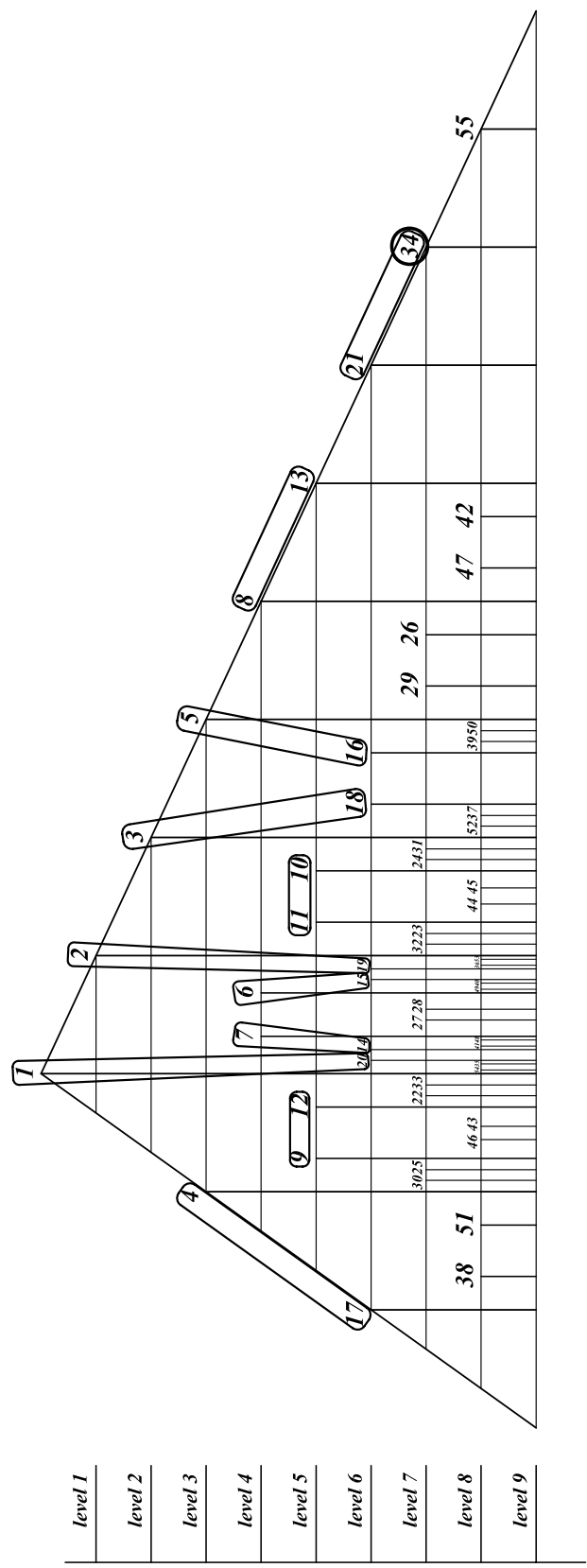


Figure 18: Building *level 8* (to be seen in landscape orientation).

